Effect of Initiation Conditions on the Uniformity of Three-Arm Star Molecular Brushes

Krzysztof Matyjaszewski* and Shuhui Qin

Center for Macromolecular Engineering, Department of Chemistry, Carnegie Mellon University, Pittsburgh, Pennsylvania 15213

Jamie R. Boyce, David Shirvanyants, and Sergei S. Sheiko*

Department of Chemistry, University of North Carolina at Chapel Hill, Chapel Hill, North Carolina 27599-3290

Received October 28, 2002; Revised Manuscript Received January 6, 2003

ABSTRACT: A series of three-arm star densely grafted molecular brushes with poly(*n*-butyl acrylate) side chains were prepared by atom transfer radical polymerization (ATRP). The three-arm macroinitiators of poly(2-bromopropionyloxyethyl methacrylate) were prepared by ATRP of 2-trimethylsilyloxyethyl methacrylate using trifunctional initiators 1,1,1-tris(4-(2-bromoisobutyryloxy)phenyl)ethane and different catalytic systems, i.e., a $Cu^{I}X$/dNbpy complex (X = Br, Cl) with and without $Cu^{II}X_2$ (X = Br, Cl) as deactivators, followed by the subsequent esterification with 2-bromopropionyl bromide. The kinetics exhibited first-order reaction with respect to the monomer concentration in all systems. Polymerization rates decreased with the catalyst in the order of CuBr > CuBr/$CuBr_2$ > CuCl > CuCl/$CuCl_2$. The different initiation conditions also affect the polydispersities of the final brushes, although in all cases the number-average molecular weight (M_n) increases with the increasing monomer conversion. AFM measurements of multiarm brushes enabled quantitative analysis of the length distribution. Because of visualization of individual starlike molecules, one could separately analyze the brush arms and the whole molecule. The polydispersities of the arm length decreased in the order of CuBr > CuBr/$CuBr_2$ > CuCl > CuCl/$CuCl_2$. The CuCl/$CuCl_2$ system seems to be the best catalyst for the star synthesis yielding brushes with narrow length distribution. CuBr is a relative "worst" catalyst system in which several coupled molecular brushes were observed, while some arms were missing. These led to the broadest distribution of arm length. Similar analysis for four-arm molecular brushes was performed. The polydispersity of the total length was significantly lower than those of the arm length. Here, the total length polydispersity displayed amazing agreement with Schulz−Flory theory for chain coupling.

Introduction

One of the main goals in modern synthetic polymer chemistry is to prepare polymers with controlled molecular weight and well-defined architecture.[1] Living polymerizations developed in the past 40 years, including carbanionic, carbocationic, and ring-opening polymerizations, help to reach these goals. However, one of the major drawbacks of living ionic polymerizations preventing them from wider industrial application is that the stringent polymerization conditions are required. Free radical polymerization is the most important industrial process to produce various vinyl polymers, but conventional free radical polymerization methods lack the control because of chain transfer and termination processes.[2,3] This precludes conventional radical polymerization from allowing the synthesis of well-defined polymers with low polydispersities and complex architecture.

Controlled/living radical polymerization (CRP) provides access to polymers with controlled molecular weight and narrow molecular weight distributions and with various architectures.[3−5] Atom transfer radical polymerization (ATRP) is among the most efficient CRP methods and has been successfully applied to the synthesis of linear, (hyper)branched, comblike, and starlike structures.[6−16]

Densely grafted molecular brushes are among the most intriguing macromolecular structures and can be synthesized by "grafting onto", "grafting through", and "grafting from" methods.[17−19] ATRP has been successfully used to prepare molecular brushes with either methacrylate or polystyrene backbones and various polyacrylates and polymethacrylate and poly(ethylene oxide) side chains by using the "grafting from" approach.[20−25] In addition, side chains with block copolymer structures have been prepared.[21,22] The molecular brushes are so large that they can be visualized as single molecules by AFM, and in addition, they are subject to various phase transitions induced by external stimuli, such as pressure.[26,27]

In this study, we reported on the first preparation of nonlinear brushes with a shape of three- and four-arm stars. They were prepared using the starlike backbone made by ATRP and subsequent grafting-from poly(*n*-butyl acrylate) by ATRP as shown in Scheme 1. A series of three-arm star brushes were synthesized using different catalyst systems. The effect of initiation conditions on the polydispersity of the arm length and of the total length was studied by AFM. In addition, four-arm star molecular brushes with similar composition were prepared and analyzed.

Experimental Section

Materials. 2-(Trimethylsilyloxyl)ethyl methacrylate (HEMA-TMS), 1,1,1-tris(4-(2-bromoisobutyryloxy)phenyl)ethane (3Br^{i}Bu), and pentaerythritol tetrakis(2-bromoisobutyrate) (4Br^{i}Bu) were synthesized according to procedures reported in the literature.[16,28] *n*-Butyl acrylate (*n*BuA) (Aldrich, 98%) was dried over calcium hydride and then distilled under reduced pressure. Copper(I) bromide (Cu(I)Br) (Acros, 98%) and copper-

10.1021/ma021633w CCC: $25.00
Published on Web 02/22/2003

Scheme 1. Synthesis of Three- and Four-Arm Star Molecular Brushes

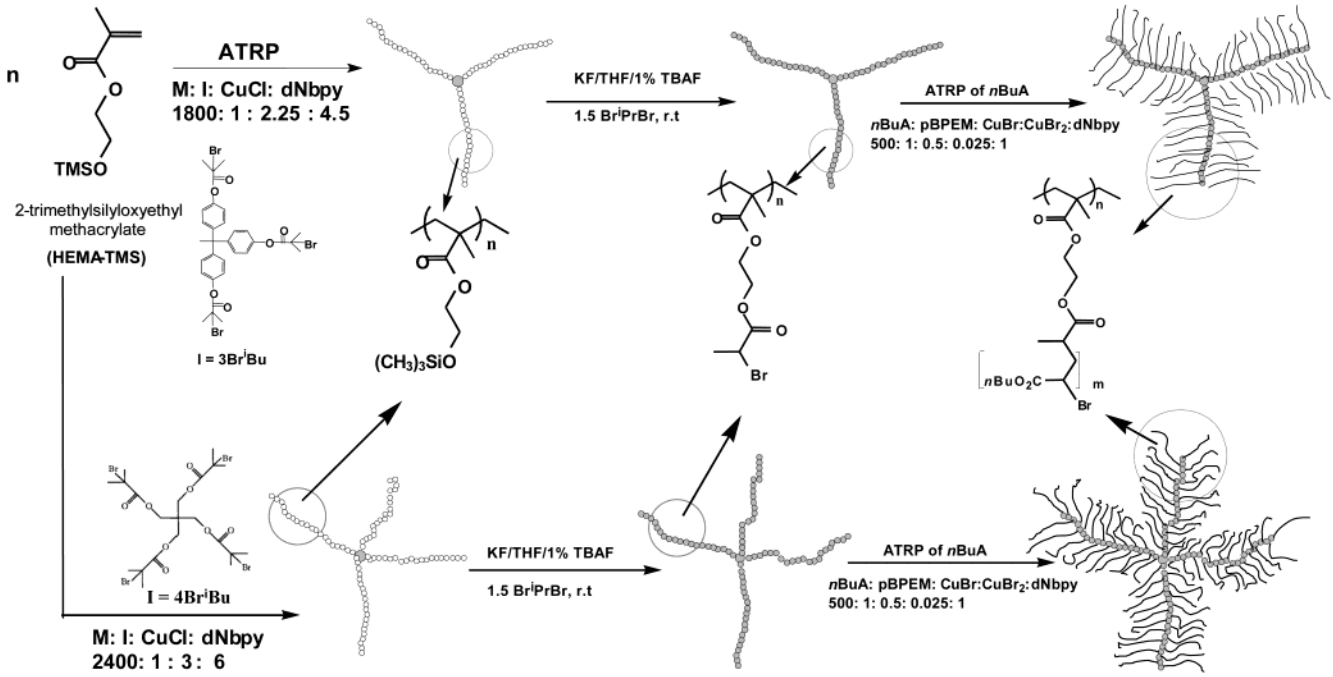

(I) chloride (Cu(I)Cl) (Acros, 99%) were purified by washing with glacial acetic acid, followed by absolute ethanol and acetone, and then dried under vacuum. Copper(II) bromide ($Cu(II)Br_2$) (Aldrich, 99%) and copper(II) chloride ($Cu(II)Cl_2$) (Aldrich, 99+%) were used as received. 4,4′-Di(5-nonyl)-2,2′-bipyridine (dNbpy) was prepared as described elsewhere.[29] All other regents and solvents were used as received from Aldrich or Acros Chemicals.

Measurements. Monomer conversion of HEMA-TMS and *n*BuA was determined using a Shimadzu GC 14-A gas chromatograph equipped with a FID detector using a J&W Scientific 30m DB WAX Megabore column. Injector and detector temperatures were kept constant at 250 °C with a heating rate of 20 °C/min. (Co)polymer molecular weights were determined using a GPC system equipped with a Waters WISP 712 autosampler and Polymer Standards Service columns (guard, 10^2 Å, 10^3 Å, 10^5 Å); toluene was used as an internal standard for the system. ^{1}H NMR characterization was performed in $CDCl_3$ (using $CHCl_3$ $\delta = 7.24$ ppm as an internal standard) on a Bruker 300 MHz instrument. Atomic force micrographs were recorded with a Multimode Nanoscope IIIa instrument (Veeco Metrology Group, Santa Barbara, CA) operating in the tapping mode. The measurements were performed at ambient conditions using Si cantilevers with a spring constant of ca. 50 N/m and a resonance frequency of about 300 kHz. The samples for tapping mode AFM measurements were prepared by the Langmuir−Blodgett technique as described in ref 27. For every sample, monolayers were transferred to a mica substrate at the same surface pressure $\pi = 1$ mN/m.

Synthesis of Three-Arm Star Molecular Brushes. All the polymerizations including the star macroinitiators and corresponding brushes were synthesized via similar procedures, unless specified otherwise. Typical procedures of three-arm star pHEMA-TMS, three-arm star pBPEM and corresponding three-arm star brushes were as follow.

Synthesis of Three-Arm Star pHEMA-TMS. In a 25 mL dried Schlenk flask 3Br^{i}Bu (10.3 mg, 0.0137 mmol) and dNbpy (25.3 mg, 0.062 mmol) were purged three times with inert gas. Deoxygenated HEMA-TMS (5.0 g, 24.71 mmol) and 1.5 mL of anisole were then added, and the reaction mixture was degassed by three freeze−pump−thaw cycles. After stirring for 1 h at room temperature (rt), Cu(I)Cl (3.06 mg, 0.031 mmol) was added, and the flask was placed in a thermostated oil bath at 75 °C. After 2 min, an initial kinetic sample was taken. Samples were removed to analyze conversion by GC and analyze molecular weight by GPC in different time intervals during the polymerization. After 12.5 h, the polymerization was stopped at 51.6% conversion by cooling to rt and opening the flask to air. The mixture was then dissolved into 50 mL of THF and passed through neutral alumina; the solvent and the residual monomer were removed using high vacuum.

Esterification of Three-Arm Star pHEMA-TMS to Three-Arm pBPEM. The product of the pHEMA-TMS polymer was placed in a 250 mL round-bottom flask (assuming 12.7 mmol of R−OTMS groups). After KF (0.74 g, 12.7 mmol) addition, the flask was sealed and flushed with N_2, and 120 mL of dry THF was added. Tetrabutylammonium fluoride (0.034 g, 0.13 mmol) in tetrahydrofuran was added dropwise to the flask, followed by the slow addition of 2-bromopropionyl bromide (4.12 g, 2.0 mL, 19.1 mmol) over the course of 40 min. The reaction mixture was stirred overnight at rt and afterward precipitated into methanol/ice (80/20 v/v %). The separated precipitate was redissolved in 150 mL of $CHCl_3$ and filtered through a column of activated alumina (basic), and the solvent was removed in a vacuum. The isolated polymer was reprecipitated from THF into hexanes three times and dried under vacuum at 25 °C for 24 h. 2.2 g of three-arm star pBPEM was obtained (65.6% yield). Complete conversion was determined by ^{1}H NMR (absence of TMS−O− resonance ($\delta = 0.2$ ppm (9H, bs, $(H_3C)_3$-Si−))). M_n(GPC) = 90 200; $M_w/M_n = 1.15$. ^{1}H NMR (300 MHz, $CDCl_3$, δ in ppm): 4.52 (1H, quart., $J = 6.8$ Hz, Br−C*H*−CH_3); 4.36 (2H, bs, −O−CH_2−CH_2−O−CO−CH−Br); 4.15 (2H, bs, −O−CH_2−CH_2−O−CO−CH−Br); 1.82 (overlapped, d, $J = 6.8$ Hz, Br−CH−CH_3); 2.21−1.44 (overlapped, m, CH_2−C−CH_3); 1.22−0.94 (overlapped, 3 × bs, CH_2−C−CH_3).

Three-Arm Star Molecular Brushes. In a 100 mL Schlenk flask pBPEM (0.1 g, 0.38 mmol of initiating sites), $CuBr_2$ (2.12 mg, 0.0095 mmol), and dNbpy (154.5 mg, 0.38 mmol) were purged three times with inert gas. Deoxygenated *n*BuA (24.3 g, 0.19 mol) and anisole (6.8 mL, 25 v%) were added, and the reaction mixture was degassed by three freeze−pump−thaw cycles. After stirring for 1 h at rt, CuBr (27.2 mg, 0.19 mmol) was added, and the flask was placed in a thermostated oil bath at 70 °C. After 2 min, an initial kinetic sample was taken, and samples were removed to analyze conversion by GC using anisole as internal standard and analyze molecular weight by GPC during the polymerization. The polymerization was stopped at 6.2% conversion after 42 h by cooling to rt and opening the flask to air. The polymer was purified by distilling

Table 1. Experimental Conditions and Kinetic Results for Three-Arm pHEMA-TMS Synthesis

	catalyst, temp	k_p^{app}, 10^5 s^{-1}	$k_{P\bullet}$,[c] 10^{-3} L mol^{-1} s^{-1}	[P•], 10^8 mol L^{-1}
I_A[a]	$CuCl/CuCl_2$, 75 °C	0.83	1.11	0.75
I_B[b]	CuCl, 75 °C	1.57	1.11	1.41
I_C[a]	$CuBr/CuBr_2$, 70 °C	2.21	1.00	2.21
I_D[b]	CuBr, 70 °C	3.40	1.00	3.40

[a] [HEMA-TMS]:[3Br^{i}Bu]:[Cu(I)]:[Cu(II)]:[dNbpy] = 1800:1:2.25:0.45:4.5. [b] [HEMA-TMS]:[3Br^{i}Bu]:[Cu(I)]:[Cu(II)]:[dNbpy] = 1800:1:2.25:0:4.5. [c] $\ln(k_{P\bullet}) = 14.685 - 2669/T$. See: Hutchinson, R. A.; Aronson, M. T.; Richards, J. R. *Macromolecules* **1993**, *26*, 6410.

Table 2. SEC Data for Three-Arm PBPEM Backbone Macroinitiators

	three-arm pHEMA-TMS		three-arm pBPEM	
	M_n	M_w/M_n	M_n	M_w/M_n
I_A	8.40×10^4	1.14	9.13×10^4	1.15
I_B	8.27×10^4	1.16	9.02×10^4	1.16
I_C	8.54×10^4	1.17	9.25×10^4	1.18
I_D	9.32×10^4	1.19	9.78×10^4	1.21

off both the solvent and the monomer under high vacuum at rt, dissolving the crude polymer in methylene chloride (about 100 mL), and passing it through an alumina column, followed by removing the solvent on a rotary evaporator (25 °C) and drying the product in high vacuum at rt for 24 h. Yield: 1.61 g of isolated polymer ($DP_{sc,grav} = 30$).

Using similar approaches, a series of three-arm star brushes were synthesized using different catalytic systems, i.e., $CuCl/CuCl_2$, CuCl, $CuBr/CuBr_2$, and CuBr. The detailed conditions and results are compiled in Tables 1 and 2.

Synthesis of Four-Arm Star Molecular Brushes. All the procedures are the same as that of three-arm star brushes I_B synthesis; the only difference is 4Br^{i}Bu was used as initiator during the backbone macroinitiator synthesis. After esterification reaction and growing *n*BuA from the four-arm star backbone macroinitiator, the four-arm star molecular brushes with $DP_{arm} = 300$ and $DP_{sc,grav} = 37$ were obtained.

Results and Discussion

Synthesis of Three-Arm Star Molecular Brushes—Effect of Initiation Conditions on the Uniformity of the Brushes. A series of three-arm star densely grafted molecular brushes were synthesized by ATRP of *n*BuA from three-arm star backbone macroinitiators. The macroinitiators were prepared by ATRP of HEMA-TMS initiated with 1,1,1-tris(4-(2-bromoisobutyryloxy)-phenyl)ethane (3Br^{i}Bu) under different catalytic systems, followed by the esterification with 2-bromopropionyl bromide (Scheme 1). The catalytic systems used in ATRP of HEMA-TMS were complexes of dNbpy with $CuCl/CuCl_2$, CuCl, $CuBr/CuBr_2$, and CuBr. They affected not only the kinetics of polymerization but also the polydispersities of the backbones and those of the final brushes.

The ATRP of HEMA-TMS was carried out in anisole. Except for slightly different temperature, all other conditions were similar in four catalytic systems as shown in Table 1. Figure 1 shows the relationships of $\ln([M]_0/[M])$ vs time for these four polymerizations. As seen, the semilogarithmic plots all linear and pass through the origin. This means the concentration of growing radicals is constant during the polymerization in all systems, confirming the first-order kinetics in monomer concentration under all reaction conditions. However, the polymerization rates were quite different, as shown in Figure 1. They decreased with the catalyst in order CuBr > $CuBr/CuBr_2$ > CuCl > $CuCl/CuCl_2$. The

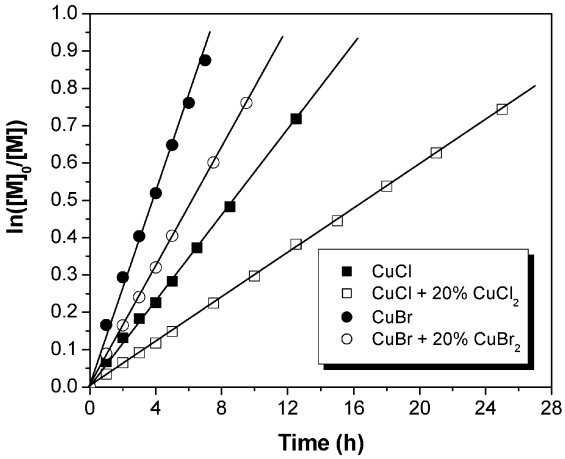

Figure 1. Dependence of $\ln([M]_0/[M])$ on time in the polymerization of HEMA-TMS using different initiation conditions. Conditions are shown in Table 1.

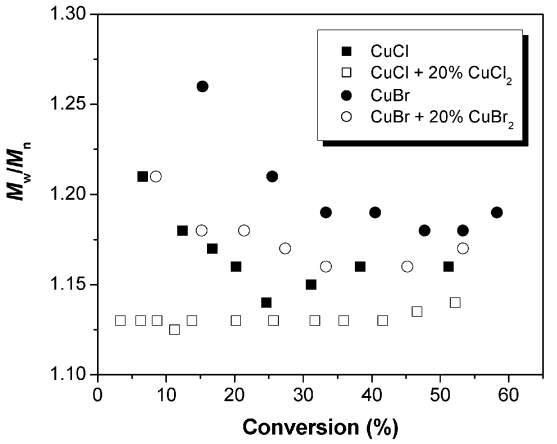

Figure 2. Dependence of M_w/M_n on conversion in the polymerization of HEMA-TMS using different initiation conditions. Conditions are the same as in Figure 1.

apparent propagation rate constants (k_p^{app}) in these polymerizations were calculated from the slopes of the straight lines plotted in Figure 1. The stationary concentration of radicals [P•] was then estimated from the ratio of the apparent propagation rate constant and the rate constants of radical propagation available, i.e., $[P^\bullet] = k_p^{app}/k_{P\bullet}$.[30,31] The kinetic data and the estimated concentrations of growing radicals are compiled in Table 1. The different polymerization rates are due to the different concentrations of the stationary concentration of growing radicals [P•] in the system. In addition, the effect of different initiation conditions on the level of the control of polymerization is significant. Figure 2 shows the evolution of polydispersities with conversion in these four polymerization systems. $CuCl/CuCl_2$ seems to be the best catalyst for the star synthesis; the polydispersities stay low from the beginning (M_w/M_n = 1.13) and fluctuate less throughout polymerization, indicating the "halogen exchange" and addition of Cu(II) improved the control of the polymerization. In other cases, the polydispersities were relatively higher than that of $CuCl/CuCl_2$ catalyst system at the beginning of the polymerization. However, all the values decreased with conversion according to equation $M_w/M_n = 1 + (k_p[I]_0/k_d[Cu^{II}])(2/P - 1)$.[11] The polydispersities for the final products of three-arm star pHEMA-TMS were 1.19 (CuBr), 1.17 ($CuBr/CuBr_2$), 1.16 (CuCl), and 1.14 ($CuCl/CuCl_2$), indicating the degree of control

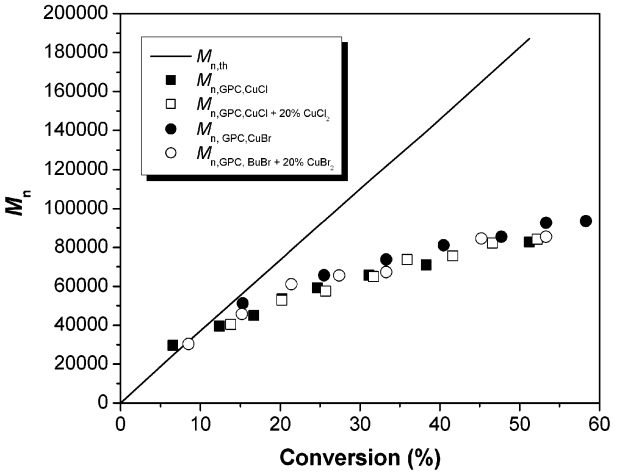

Figure 3. Dependence of M_n on conversion in the polymerization of HEMA-TMS using different initiation conditions. Conditions are the same as in Figure 1.

of polymerization was higher with halogen exchange[32,33] and in the presence of Cu(II). The overall control level is $CuCl/CuCl_2$ > CuCl > $CuBr/CuBr_2$ > CuBr. Figure 3 shows the number-average molecular weights of three-arm star pHEMA-TMS increased with increasing monomer conversion in all systems; however, the values were lower than the theoretical ones calculated by $M_n = MW \times (\Delta[M]/[I]_0)$. This can be due to the more compact structure of three-arm stars than linear polymers and different hydrodynamic volumes of pHEMA-TMS from linear pMMA standards.

All the esterification reactions were performed in a similar way, i.e., by reaction with 2-bromopropionyl bromide in situ using KF/tetrabutylammonium fluoride as catalyst in THF. The purified three-arm pBPEM macroinitiators were characterized by ^{1}H NMR spectroscopy and GPC. The ^{1}H NMR spectra showed the complete transformation of pHEMA-TMS to pBPEM in all samples by the absence of Me_3Si- signals. The GPC was calibrated with pMMA standards, and the values before and after esterification are listed in Table 2. They show that the M_n increased after esterification in all cases. The polydispersities increased slightly by comparison with those of the original three-arm star pHEMA-TMS. Figures 4−7 present the overlaid GPC traces, in which all the esterified products shifted entirely to high molecular weight and no significant tailing or shoulder can be observed, indicating negligible contributions of side reactions during the esterifications. A series of three-arm star molecular brushes were synthesized by grafting *n*BuA from aforementioned macroinitiators (Scheme 1). Data of the M_n and M_w/M_n for the final brushes are compiled in Table 3, and the overlaid GPC traces are shown in Figures 4−7. The apparent molecular weight (based on pMMA standards) of the final brushes increased dramatically in all cases, and polydispersities were relatively low. As shown in Figures 4−7, all the GPC traces shifted toward higher molecular weight by comparison with the backbone macroiniators, without shoulders or tailing which indicated no evidence for brush−brush coupling reaction. The DP of p*n*BuA side chains was 38 ($CuCl/CuCl_2$), 30 (CuCl), 42 ($CuBr/Br_2$), and 33 (CuBr). The length was sufficient to extend on a mica surface and to be visualized by AFM.

AFM Characterization of the Three-Arm Star Brushes. The amphiphilic structure of *n*-butyl acrylate groups led to spontaneous spreading of p*n*BuA brushes on the water surface to form a dense monolayer upon compression.[27] To visualize individual molecules, monolayers were transferred to a mica substrate and scanned by AFM. Figure 8a shows a large-scale image of polymer I_A prepared using $CuCl/CuCl_2$ as catalyst. The image demonstrates a fairly uniform structure of the transferred monolayers in which individual molecules are

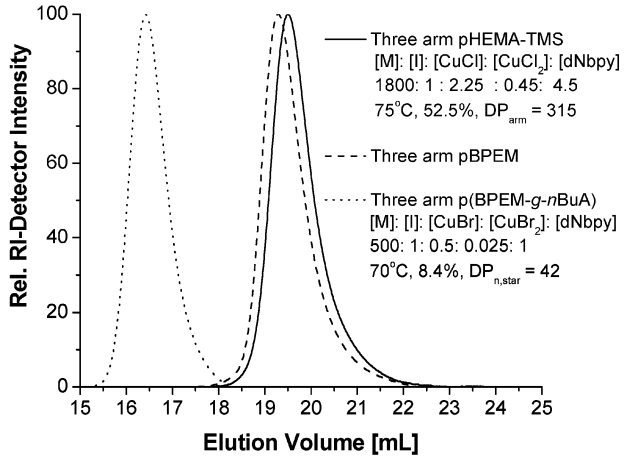

Figure 4. GPC traces during the syntheses of three-arm star pBPEM-*g*-p*n*BuA molecular brushes; $CuCl/CuCl_2$ was used as catalyst during the backbone synthesis.

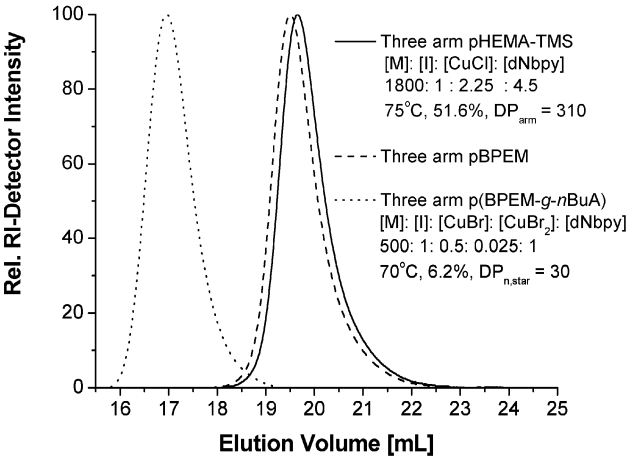

Figure 5. GPC traces during the syntheses of three-arm star pBPEM-*g*-p*n*BuA molecular brushes; CuCl was used as catalyst during the backbone synthesis.

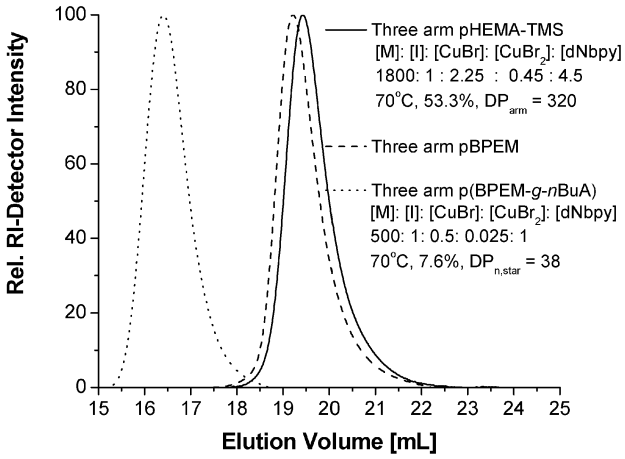

Figure 6. GPC traces during the syntheses of three-arm star pBPEM-*g*-p*n*BuA molecular brushes; $CuBr/CuBr_2$ was used as catalyst during the backbone synthesis.

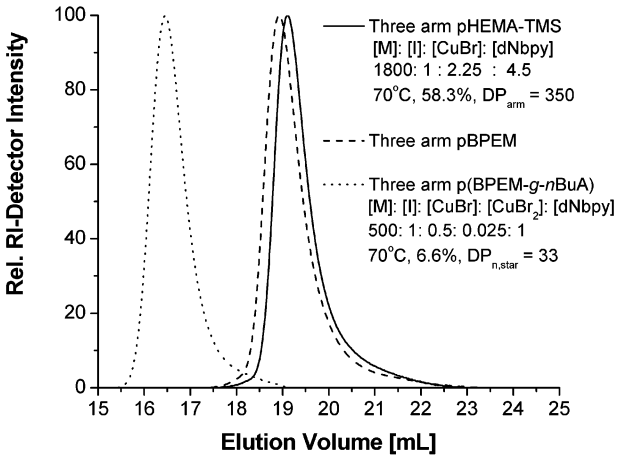

Figure 7. GPC traces during the syntheses of three-arm star pBPEM-*g*-p*n*BuA molecular brushes; CuBr was used as catalyst during the backbone synthesis.

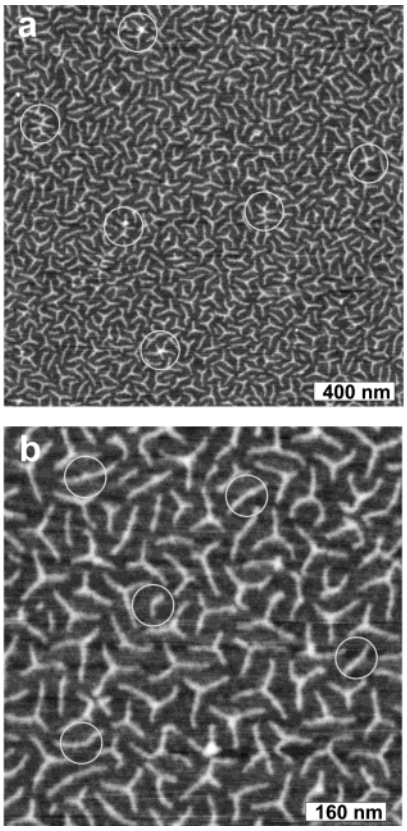

Figure 8. AFM images of three-arm star pBPEM-*g*-p*n*BuA brushes; CuCl/CuCl$_2$ was used as catalyst during the backbone synthesis. (a) Large scale image; circles show molecular overlapping. (b) Zoomed image; circles show linear molecules.

Table 3. Experiment SEC and Gravimetric Results of the Final Three-Arm Brushes

	$M_{n,app}$	M_w/M_n	DP_{arm}	DP_{sc}
I_A	5.72×10^5	1.19	315	38
I_B	4.76×10^5	1.21	310	30
I_C	7.12×10^5	1.23	320	42
I_D	6.02×10^5	1.31	350	33

clearly resolved as densely packed three-arm stars with extended arms. Most of the molecules do not overlap and contain all three arms. As depicted by circles in Figure 8a, only few molecules displayed overlapping. The latter could occur either during adsorption or due to coupling reactions. Some of the molecules did not contain the third arm (Figure 8b). In this case, an undulation in the molecular contour was identified as the branching center whereas the length of the third arm was taken as zero.

Clear visualization of the arm ends enabled quantitative investigation of the arm-length distribution. Certain steps were undertaken to increase reliability and accuracy of the statistical analysis. First, all molecules in a certain image were analyzed regardless their size and shape. Only molecules at the image boarder were skipped from the analysis. This measure prevents visual discrimination of the molecules by an operator. Second, approximately 300 molecules, i.e., 900 arms, were taken for the statistical analysis. This number assured a relative standard deviation below 5%. Third, the experimental error was evaluated by performing several measurements of the same sample at different places for different scan areas. Thus, the average values and standard deviations were determined.

Figure 9a−d shows a series of tapping mode micrographs (height images) obtained from polymers I_A, I_B, I_C, and I_D. Although the images look very similar, the number of visible imperfections increases from the I_A to I_D samples. More linear and short molecules as well as dimers were observed for sample I_D in Figure 9d. This observation is consistent with the molecular weight distributions in Figure 7. The number- and weight-average lengths of brush arms as well as of the whole molecule are depicted in Table 4.

One can see that the polydispersity steadily decreases from the CuCl/CuCl$_2$ to CuBr the system. Moreover, the length polydispersity of the whole molecule decreases according to the equation

$$PDI_{brush} = \frac{PDI_{arm}}{f} + \frac{f-1}{f}$$

where f is the number of arms and $PDI = L_w/L_n$. The equation was derived on the basis of the early treatment of the statistics of chain coupling by Schulz and Flory.[34,35] The statistics describes molecular weight distribution of f-mers obtained by random linking of polydisperse linear chains with the polydispersity index PDI_{arm}. For $f = 3$ (three-arm stars with $PDI_{arm} = 1.15$), the equation gives the theoretical value $PDI_{theo} = 1.05$. The experimental PDI values in Table 4 demonstrate the amazingly good agreement with the Schulz−Flory theory.

The observation of missing arms in brushes, despite low overall polydispersity, may raise a question about efficiency of initiation for the side chains. However, it has been previously observed that the DP of side chains measured after cleavage from the backbone was within <5% of the values predicted from monomer conversion and assuming quantitative initiation.[21] Thus, majority of side chains (>95%) grow to form densely grafted molecular brushes.

Synthesis and AFM Characterization of Four-Arm Star Molecular Brushes. Similarly, four-arm star pBPEM-*g*-p*n*BuA molecular brushes were synthesized by grafting *n*BuA from pBPEM macroinitiator. The backbone macroinitiator was synthesized by ATRP of HEMA-TMS using the tetrafunctional initiator pentaerythritol tetrakis(2-bromoisobutyrate) (4Br^{i}Bu), followed by esterification of the backbone macroinitiator precursor with 2-bromopropionyl bromide. The procedures for the synthesis of four-arm star macroinitiator and brushes are presented in Scheme 1; the results are compiled in Table 5 and Figure 10.

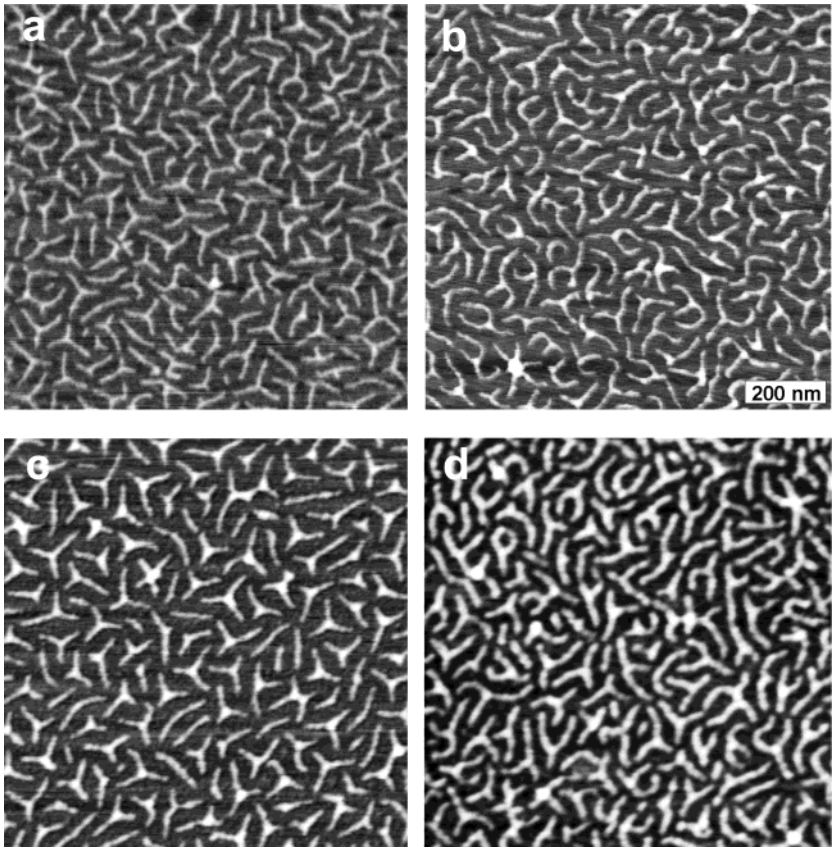

Figure 9. AFM images (1 × 1 μm) of three-arm star pBPEM-*g*-p*n*BuA brushes. Catalyst system: (a) CuCl/$CuCl_2$, (b) CuCl, (c) CuBr/$CuBr_2$, and (d) CuBr.

Table 4. AFM Results of the Final Three-Arm Brushes

	DP_{arm}	$L_{n(nm, arm)}$	$L_{w(nm, arm)}$	PDI_{arm}	$L_{n(nm, brush)}$	$L_{w(nm, brush)}$	PDI_{brush}	$PDI_{brush,theo}$[a]
I_A	315	49.2	56.1	1.14	147.9	155.0	1.048	1.047
I_B	310	55.0	58.0	1.15	165.0	173.0	1.05	1.050
I_C	320	51.5	60.3	1.17	154.6	163.2	1.06	1.057
I_D	350	60.5	72.1	1.19	182.2	195.6	1.07	1.063

[a] Calculated from the equation $PDI_{brush} = PDI_{arm}/f + (f - 1)/f$, where f is the number of arms.[34,35]

Table 5. Data for Four-Arm Star Molecular Brushes Syntheses

reaction	$M_{n,GPC}$	M_w/M_n	$DP_{each\ arm}$
four-arm pHEMA-TMS	1.04×10^5	1.16	300
four-arm pBPEM	1.20×10^5	1.16	300
four-arm pBPEM-*g*-p*n*BuA	8.05×10^5	1.37	300*37

The ATRP of HEMA-TMS initiated with 4Br^{i}Bu was carried out in anisole with CuCl/dNbpy catalyst system at 75 °C. The polymerization was stopped after 32 h, and monomer conversion was determined to be 50.1% by GC. The molecular weight and molecular weight distribution of the final four-arm star pHEMA-TMS (determined by GPC using PMMA standards) are $M_n = 1.04 \times 10^5$ and $M_w/M_n = 1.16$, respectively, as shown in Table 5.

The esterification reaction was performed using a similar approach as described for the synthesis of three-arm star pBPEM. The GPC traces of the four-arm pBPEM macroinitiator shifted entirely to high molecular weight by comparison with that of four-arm pHEMA-TMS as shown in Figure 10. No shoulders were observed, indicating negligible contributions of side reactions. The average molecular weight and molecular weight distribution of the final four-arm star pBPEM backbone macroinitiator are $M_n = 1.20 \times 10^5$ and $M_w/M_n = 1.16$ (based on pMMA standards), respectively, as summarized in Table 5.

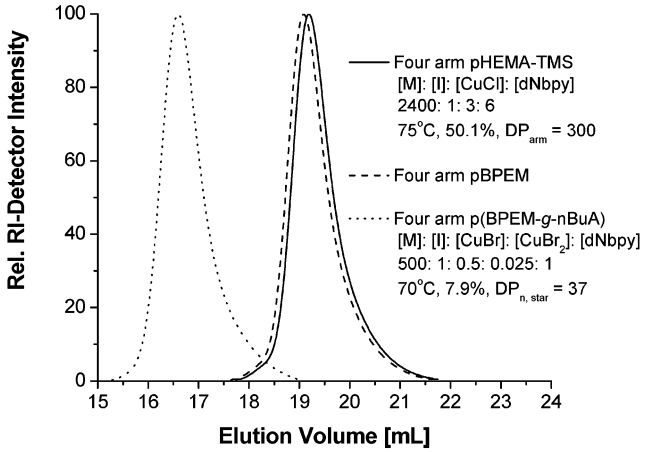

Figure 10. GPC traces during the syntheses of four-arm star pBPEM-*g*-p*n*BuA molecular brushes; CuCl was used as catalyst during the backbone synthesis.

The polymerization of *n*BuA was initiated with aforementioned four-arm pBPEM macroinitiator and resulted in four-arm star molecular brushes as shown in Scheme 1. Figure 10 shows the shifting of GPC traces

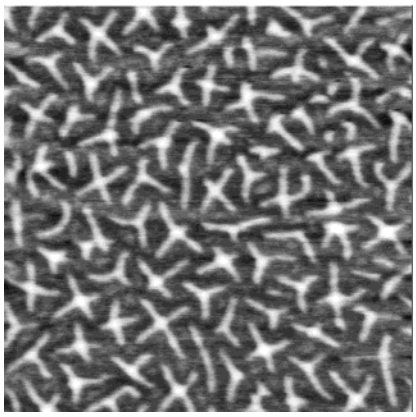

Figure 11. AFM images ($1 \times 1\ \mu$m) of four-arm star pBPEM-*g*-p*n*BuA brushes; CuCl was used as catalyst during the backbone synthesis.

of the final brushes toward higher molecular weight compared with that of macroinitiator. No shoulder formation in GPC trace indicates the successful synthesis of the brushes and no evidence for brush−brush coupling reaction during the polymerization. The apparent molecular weight (based on pMMA standards) was $M_{n,app} = 8.05 \times 10^5$, and M_w/M_n was 1.37 for the final brushes. The DP of p*n*BuA side chains was 37 by the gravimetric analysis.

Figure 11 shows an AFM micrograph of the four-arm brush molecules. Most of the molecules have four arms; however, also two- and three-arm molecules exist. The length distribution of the four-arm brushes was measured in the same way as for the three-arm molecules. The number- and weight-average lengths of arms were determined to be 64 and 74 nm, respectively. This gives a polydispersity index of 1.15, which is similar to that of the three-arm molecules. For the total length, we determined $L_n = 256$ nm, $L_w = 266$ nm, and PDI = 1.04. The latter again agrees well with the theoretical value $PDI_{theo} = 1.038$ calculated for a four-arm star.

Conclusions

Densely grafted molecular brushes with three- and four-arm star architectures were synthesized by ATRP using "grafting from" methods. The synthesized star brushes are of high molecular weight and relatively low polydispersities. AFM demonstrated that the molecular brushes, adsorbed on the mica surface, have a wormlike structure, and all arms are extended due to the strong interaction between the polar *n*BuA units and the polar mica substrate. The detailed studies on the three-arm star brushes indicated that the initiation conditions affected not only the kinetics of polymerization but also the polydispersities of the final brushes in the order of $CuCl/CuCl_2 < CuCl < CuBr/CuBr_2 < CuBr$. In the $CuCl/CuCl_2$ catalyst system, almost all the brushes have three arms and similar arm length. In the CuBr catalyst system, more coupled molecular brushes were observed, and some arms were missing, leading to the broadest distribution of arm length. The kinetic experimental observations, coupled with AFM results, lead to some general "rules" by which the well-defined three-arm star brushes can be achieved.

Acknowledgment. This work was financially supported by the National Science Foundation (ECS-01-03307) and CRP Consortium members at Carnegie Mellon University.

References and Notes

(1) Webster, O. W. *Science* **1991**, *251*, 887.
(2) Moad, G., Solomon, D. H., Eds. *The Chemistry of Free-Radical Polymerization*; Pergamon: Oxford, UK, 1995.
(3) Matyjaszewski, K., Davis, T. P., Eds. *Handbook of Radical Polymerization*; John Wiley & Sons: Hoboken, 2002.
(4) Matyjaszewski, K., Ed. *Controlled Radical Polymerization;* ACS Symp. Ser. 685; American Chemical Society: Washington, DC, 1998.
(5) Matyjaszewski, K., Ed. *Controlled/Living Radical Polymerization. Progress in ATRP, NMP, and RAFT;* ACS Symp. Ser. 768; American Chemical Society: Washington, DC, 2000.
(6) Wang, J. S.; Matyjaszewski, K. *J. Am. Chem. Soc.* **1995**, *117*, 5614.
(7) Davis, K. A.; Matyjaszewski, K. *Adv. Polym. Sci.* **2002**, *159*, 1.
(8) Matyjaszewski, K. *Chem.—Eur. J.* **1999**, *5*, 3095.
(9) Patten, T. E.; Matyjaszewski, K. *Acc. Chem. Res.* **1999**, *32*, 895.
(10) Patten, T. E.; Matyjaszewski, K. *Adv. Mater.* **1998**, *10*, 901.
(11) Matyjaszewski, K.; Xia, J. H. *Chem. Rev.* **2001**, *101*, 2921.
(12) Kamigaito, M.; Ando, T.; Sawamoto, M. *Chem. Rev.* **2001**, *101*, 3689.
(13) Zhang, X.; Xia, J. H.; Matyjaszewski, K. *Macromolecules* **2000**, *33*, 2340.
(14) Wang, J. S.; Greszta, D.; Matyjaszewski, K. *ACS Polym. Mater. Eng.* **1995**, *73*, 416.
(15) Coessens, V.; Pintauer, T.; Matyjaszewski, K. *Prog. Polym. Sci.* **2001**, *26*, 337.
(16) Matyjaszewski, K.; Miller, P. J.; Pyun, J.; Kickelbick, G.; Diamanti, S. *Macromolecules* **1999**, *32*, 6526.
(17) Tsukahara, Y.; Tsutsumi, K.; Yamashita, Y.; Shimada, S. *Macromolecules* **1990**, *23*, 5201.
(18) Schappacher, M.; Deffieux, A. *Macromolecules* **2000**, *33*, 7371.
(19) Dziezok, P.; Sheiko, S. S.; Fischer, K.; Schmidt, M.; Moller, M. *Angew. Chem., Int. Ed. Engl.* **1997**, *36*, 2812.
(20) Beers, K. L.; Gaynor, S. G.; Matyjaszewski, K.; Sheiko, S. S.; Moller, M. *Macromolecules* **1998**, *31*, 9413.
(21) Borner, H. G.; Beers, K.; Matyjaszewski, K.; Sheiko, S. S.; Moller, M. *Macromolecules* **2001**, *34*, 4375.
(22) Cheng, G. L.; Boker, A. A.; Zhang, M. F.; Krausch, G.; Muller, A. H. E. *Macromolecules* **2001**, *34*, 6883.
(23) Borner, H. G.; Duran, D.; Matyjaszewski, K.; da Silva, M.; Sheiko, S. S. *Macromolecules* **2002**, *35*, 3387.
(24) Qin, S.; Matyjaszewski, K.; Xu, H.; Sheiko, S. S. *Macromolecules* **2003**, *36*, 605.
(25) Neugebauer, D.; Matyjaszewski, K. *Polym. Prepr. (Am. Chem. Soc., Div. Polym. Chem.)* **2002**, *43* (2), 241.
(26) Sheiko, S. S.; Moller, M. *Chem. Rev.* **2001**, *101*, 4099.
(27) Sheiko, S. S.; Prokhorova, S. A.; Beers, K. L.; Matyjaszewski, K.; Potemkin, I. I.; Khokhlov, A. R.; Moller, M. *Macromolecules* **2001**, *34*, 8354.
(28) Beers, K. L.; Boo, S.; Gaynor, S. G.; Matyjaszewski, K. *Macromolecules* **1999**, *32*, 5772.
(29) Matyjaszewski, K.; Patten, T. E.; Xia, J. H. *J. Am. Chem. Soc.* **1997**, *119*, 674.
(30) Hutchinson, R. A.; Aronson, M. T.; Richards, J. R. *Macromolecules* **1993**, *26*, 6410.
(31) Beuermann, S.; Buback, M. *Prog. Polym. Sci.* **2002**, *27*, 191.
(32) Matyjaszewski, K.; Shipp, D. A.; Wang, J. L.; Grimaud, T.; Patten, T. E. *Macromolecules* **1998**, *31*, 6836.
(33) Shipp, D. A.; Wang, J. L.; Matyjaszewski, K. *Macromolecules* **1998**, *31*, 8005.
(34) Schulz, G. V. *Z. Phys. Chem.* **1939**, *B43*, 25.
(35) Schaefgen, J. R.; Flory, P. J. *J. Am. Chem. Soc.* **1948**, *70*, 2709.

MA021633W